PETROLEUM EXPLORATION AND DEVELOPMENT
Volume 41, Issue 3, June 2014
Online English edition of the Chinese language journal

Available online at www.sciencedirect.com
ScienceDirect

Cite this article as: PETROL. EXPLOR. DEVELOP., 2014, 41(3): 365–370.

RESEARCH PAPER

Research on oil displacement mechanism in conglomerate using CT scanning method

DENG Shiguan[1,2,3,*], LÜ Weifeng[1,2], LIU Qingjie[1,2], LENG Zhenpeng[1,2], LI Tong[1,2], LIU Hongxian[4], GU Hongjun[4], XU Changfu[4], ZHANG Xuhui[3], LU Xiaobing[3]

1. State Key Laboratory of Enhanced Oil Recovery, Beijing 100083, China;
2. PetroChina Research Institute of Petroleum Exploration & Development, Beijing 100083, China;
3. Institute of Mechanics, Chinese Academy of Sciences (CAS), Beijing 100190, China;
4. Research Institute of Exploration and Development, PetroChina Xinjiang Oilfield Company, Karamay 834000, China

Abstract: Taking the conglomerate from Xinjiang Oilfield as study object, the porosity distribution characteristics of the conglomerate were analyzed with CT scanning; through the online monitoring of the water and polymer flooding process in a conglomerate core using an CT scanning system, the saturation profile along the core and the CT reconstructed images of core section during the displacing process were obtained; oil displacement mechanism was analyzed according to a new characterization parameter, "oil saturation frequency distribution". The results show that the conglomerate has strong heterogeneity, resulting in "dominant channels", and in turn ineffective water circulation and low water flooding oil recovery, moreover, the oil in high oil saturation area is produced first. In polymer flooding, the oil in high and medium oil saturation areas can be produced but the oil in low oil saturation areas still cannot be produced. Oil produced in the subsequent water flooding is still mainly from the high oil saturation areas. For conglomerate reservoirs, previous water flooding should reach as high water cut as possible so as to strengthen the slug effect of the polymer. Meanwhile the injection volume of polymer should be reduced, and a subsequent water flooding should be used to push the polymer slug to produce oil.

Key words: conglomerate; CT scanning; water flooding; polymer flooding; oil saturation; profile along the core; frequency distribution

Introduction

The conventional water flooding for conglomerate reservoirs which are characterized by intense heterogeneity and complex pore structure usually ends up with high remaining oil saturation, high water cut and low production, polymer flooding can effectively improve the recovery [1–2]. However, the mechanism of low waterflooding recovery rate and polymer flooding for conglomerate remains unclear. In the past research, core displacement experiments were mainly used to collect data at both ends of cores from which macro parameters were calculated to describe the oil displacement process, which could not reveal the displacement mechanism completely.

CT scanning technology can make up the shortcomings of the traditional method. It can make quantitative and image analysis of petrophysics, and visual characterization of pore structures; meanwhile, the saturation distribution inside the core can also be obtained from CT scanning to visualize the displacement process, and get better insight into the oil displacement mechanism [3–5]. Nowadays CT scanning, already a routine test technique in international oil industry [6–8], has been adopted in some research in China [9–11].

Taking the conglomerates from Xinjiang Oilfield as objects, CT scanning was adopted to analyze the dual-porosity structure characteristics and oil displacement mechanism of the conglomerates in the study; furthermore, a new characterization parameter was put forward based on CT scanning to compare the displacement characteristics of water flooding and polymer flooding, and a reasonable injection method for conglomerate reservoirs was put forward accordingly at last.

1 Core experiments based on CT scanning system

1.1 Experimental apparatus

CT scanning core displacement system developed by Enhanced Oil Recovery Department, Research Institute of Petroleum Exploration& Development, PetroChina was employed in this experiment. A LightSpeed 8 CT scanner from GE with a resolution scale of 0.18 mm was used as the scan-

Received date: 31 Oct. 2013; **Revised date:** 25 Feb. 2014.
*** Corresponding author.** E-mail: lweifeng@petrochina.com.cn
Foundation item: Supported by the National Key Basic Research and Development Program (973 Program), China (2011CB707302); CNPC Science and Technology Program (2011A-1003); the National High Technology Research and Development Program (863 Program), China (2009AA063403).

ning system. The cores were scanned under 120kV and 130 mA with a 1.25 mm scanning pitch. Two groups of QUIZIX 5200 pump were used as the injection system and one group of ISCO pump as the overburden pressure controlling system. A special core-holder was used, so X-ray could penetrate through and the beam hardening effect could be eliminated. This displacement system allow the scanning of the displacement process of cores with CT scanner online, and collect the flow rate and pressure at the inlet and outlet of the coreholder. Finally, Core CT Analysis Software (CCTAS1.0) was used to process the experimental data.

1.2 Core samples and fluids

LY-1 and LY-2 samples taken from Xinjiang Oilfield were used in the experiment, their petrophysical parameters are listed in Table 1. With intense heterogeneity, both samples are typical dual porosity media.

1.3 Experiment procedure

The experiments were conducted at an ambient temperature of 22 °C, an overburden pressure of 5MPa and no back pressure. The specific process was as follows: the core was placed in the core holder after drying and then scanned by CT; next, the core was vacuumized, fully saturated with simulation formation water and then scanned by CT, to get the core porosity [12] and its 2-D/ 3-D porosity distribution. Irreducible water state was established for the core with simulated oil, and then the simulated oil inside the core was replaced with degassed oil added with 5% iodohexane (reinforcing agent for CT value). Brine was injected into the LY-1, LY-2 cores at an injection rate of 0.05 mL/min (1st water flooding). The 1st water flooding of LY-1 and LY-2 ended at a water cut of 98% and 90% respectively. The core was scanned at a regular time interval during the water flooding process (a single scan took 17s), to get the saturation distribution in the course of displacement [13–14]. At last polymer solution of 0.7PV was injected, then both LY-1 and LY-2 were displaced with brine again until the water cut surpassed 98% (2nd water flooding), the saturation distribution of the core during the polymer and 2nd water flooding process was also obtained through CT scanning, and the effect of different water and polymer injection modes on recovery percent was compared.

2 Pore structure analysis of dual porosity media

The CT value of every slice of LY-1 and LY-2 exhibits a bimodal feature (Fig.1, 2 slices of LY-1). The corresponding reconstructed images of CT value distribution also show intense heterogeneity (Fig. 2).

Table 1 Petrophysical parameters of core samples

Sample No	Length/ cm	Diameter/ cm	Pore Volume/mL	Porosity/ %	K_{air}/ 10^{-3} μm^2
LY-1	5.12	3.78	16.0	27.8	1 419
LY-2	7.78	3.74	17.1	20.1	379

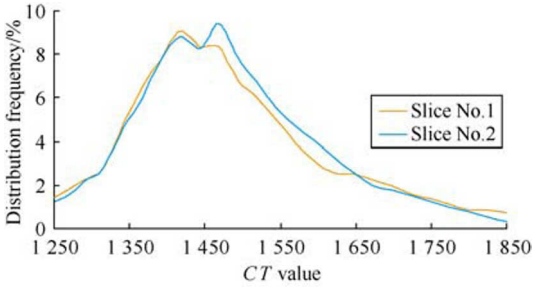

Fig. 1 CT value distribution of two slices from LY-1

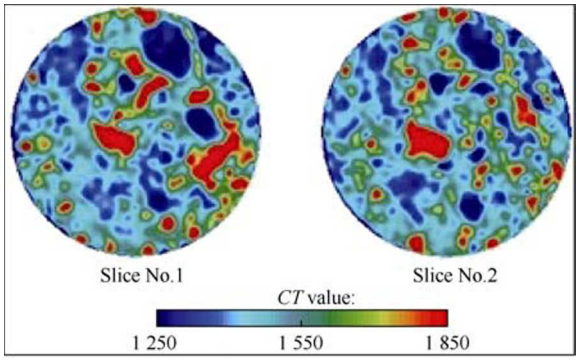

Fig. 2 CT value reconstructed images of two slices from LY-1

The porosity frequency distribution of LY-1 and LY-2 was calculated and shown in Fig. 3. It can be seen that the porosity frequency distribution of both cores exhibit a bimodal feature. 3-D reconstructed graphs of porosity distribution of both cores were derived by CCTAS and shown in Fig. 4 which reveal intense heterogeneity of the cores.

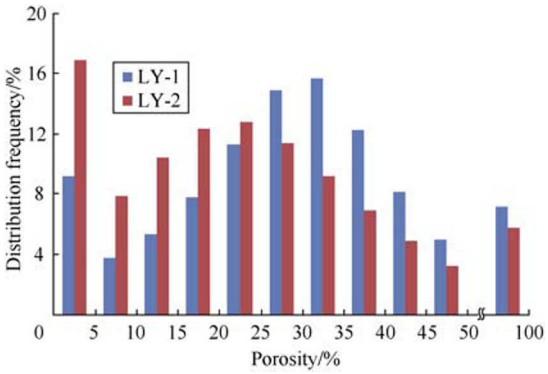

Fig. 3 Porosity distribution of LY-1 and LY-2

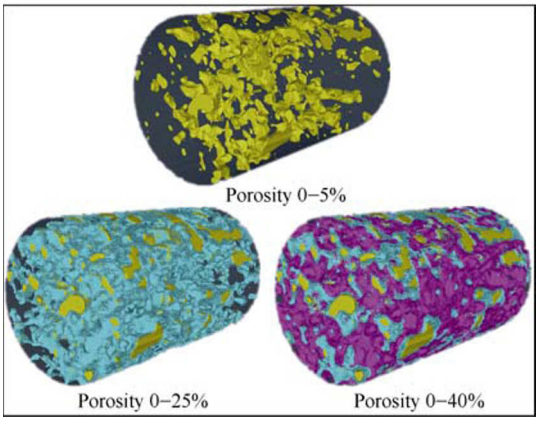

Fig. 4 3-D reconstructed images of porosity distribution for LY-1

Conglomerates are mainly composed of clastic grains and interstitial matter which differs greatly in density and pore structure. Tight clastic grains, but loose interstitial matter, coupling with different cementation degree of clastic grain and interstitial matter result in the mutil-mode and intensely heterogeneous dual-porosity structure of conglomerate, which lead to the bimodal feature of CT value and porosity frequency distribution of conglomerate.

3 Core displacement experiment and oil displacement mechanism

The 1st water flooding and polymer flooding process of LY-2 is similar to that of LY-1. So this research takes LY-1 as example.

3.1 The parameter of displacement process (oil saturation frequency)

Oil saturation frequency distribution at any time during displacement process can be obtained by CCTAS (Fig. 5). The curve can show the oil saturation distribution inside the core clearly, thus revealing the oil producing degree inside the core.

3.2 1st Water flooding

The oil saturation decrement curves (initial oil saturation minus oil saturation at any moment during displacement) along the core of LY-1 during 1st water flooding were shown in Fig. 6. The water phase broke through fast (at injection volume of about 0.125PV, 40min). After breakthrough the oil saturation decrement distribution along the core showed an overall rise trend. The CT reconstructed images of core LY-1 during 1st water flooding (Fig. 7) reveal that: the overall increase of oil saturation decrement is the result of "dominant channels" formed during 1st water flooding due to the intense heterogeneity of conglomerate and in turn ineffective water circulation. After breakthrough the produced oil was almost all from the 'dominant channels'; while the oil in the rest part of the core was hardly produced.

The oil saturation frequency distribution of LY-1 during 1st water flooding is shown in Figs. 5 and 8. The frequency of 50%–100% saturation range decreased rapidly (Fig. 8), which indicates that the oil in the saturation of 50%–100% was

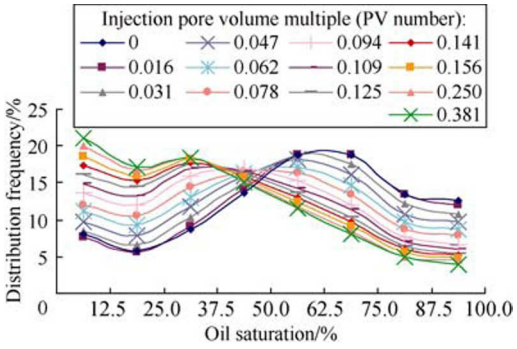

Fig. 5 Oil saturation frequency distribution curves

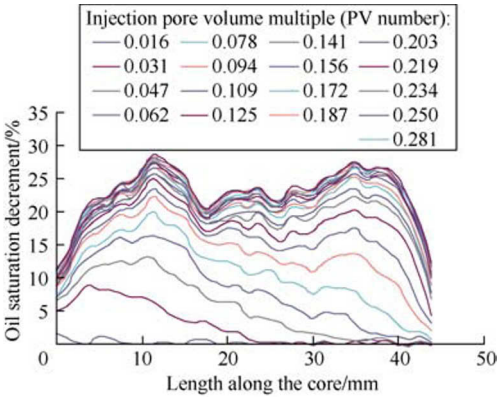

Fig. 6 Oil saturation decrement distribution along the core of LY-1 during 1st water flooding

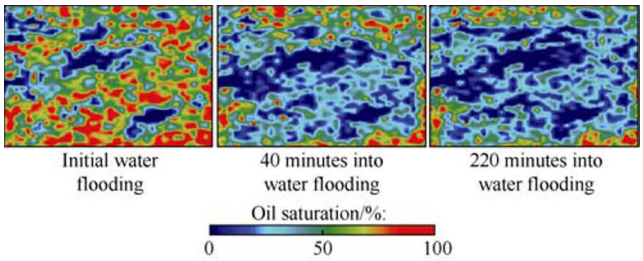

Fig. 7 CT reconstructed images of core LY-1 during 1st water flooding

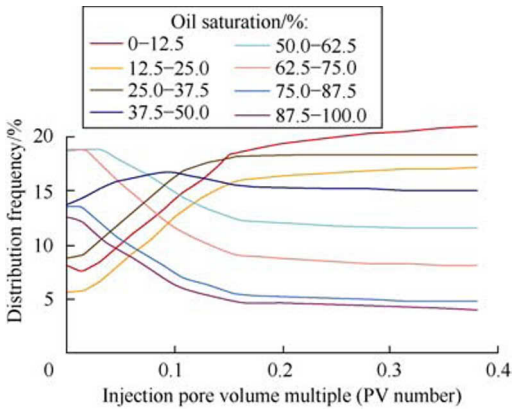

Fig. 8 Curves of oil saturation frequency for LY-1 during 1st water flooding

firstly produced. In contrast, the frequency of the saturation range 0%–25% increased quickly, because on one hand the oil in this saturation range was hard to be produced, on the other hand the water flooding residual oil saturation of other zones was in this range.

3.3 Polymer flooding

After adding iodohexane in the oil phase, the CT value difference between brine and polymer could be neglected in the calculation of oil saturation. The oil saturation decrement distribution along the core of LY-1 during polymer flooding is shown in Fig. 9. In the early stage of polymer flooding, the entire rise trend of oil saturation decrease was interrupted; in the late stage of polymer flooding, the entire rise trend of oil saturation decrease appeared again. The LY-1 CT reconstructed

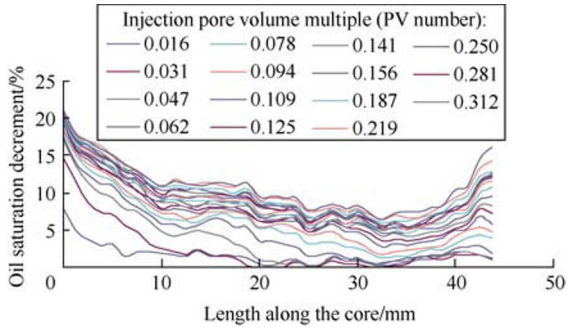

Fig. 9 Oil saturation decrement distribution along the core of LY-1 during polymer flooding

images of polymer flooding are shown in Fig. 10. It can be seen that the polymer blocked the 'dominant channels', which enabled the producing of the remaining oil of 1st water flooding (in the yellow ring of Fig. 10). Meanwhile, there was still much 'island shaped' residual oil (in the red ring of Fig. 10) cannot be produced.

The oil saturation frequency distribution of LY-1 during polymer flooding is shown in Fig. 11. Compared with that in the 1st water flooding, the middle portion of the curve (interval 37.5%–50.0%) decreases (Fig. 11a), which indicates that more oil in the saturation range of 37.5%–50% was produced than in 1st water flooding. In contrast, the change trend of the frequency of the 12.5%–37.5 % saturation range (Fig. 11b) became flat. Considering the frequency increase caused by residual oil of other zones (part of residual oil saturation of other zones was in the interval 12.5%–37.5%), the curve becoming flat indicates that the oil in the saturation range of 12.5%–37.5% was produced in polymer flooding. The frequency of the saturation range 0%–12.5% maintained the increasing trend, because on one hand the oil in this saturation range was hard to produce, on the other hand the polymer flooding residual oil saturation of other zones was in this interval.

3.4 2nd Water flooding

LY-1 hardly produced any oil during 2nd water flooding. The oil saturation decrement distribution along the core of LY-2 during 2nd water flooding still showed an overall increase trend (shown in Fig. 12), which indicates that the 2nd water flooding of LY-2 only followed the channels formed in the 1st water flooding and polymer flooding, with no new channels opened.

The oil saturation frequency distribution of LY-2 during 2nd water flooding is shown in Fig.13. It can be seen that the curve changes little with the increase of the PV number except for the frequency of the saturation range of 90%–100 %, which indicates that the produced oil of 2nd water flooding was mainly from the saturation range of 90%–100%, namely the oil that is easier to produce. These verified the conjecture that the 2nd water flooding of LY-2 only followed along the channels formed in the 1st water and polymer flooding.

4 The effect of different injection modes on the recovery percent

The recovery percent of LY-1 and LY-2 after water and polymer flooding are list in Table 2.

The 1st water flooding of LY-1 ended up with a water cut of 98%. The recovery percent of LY-1 after 1st water and polymer flooding was essentially normal. But the 2nd water flooding of LY-1 hardly produced any oil, this is because the 2nd water flooding could not push the polymer slug to produce oil due to the intense heterogeneity of the conglomerate. Based on this situation, the polymer injection PV number should be

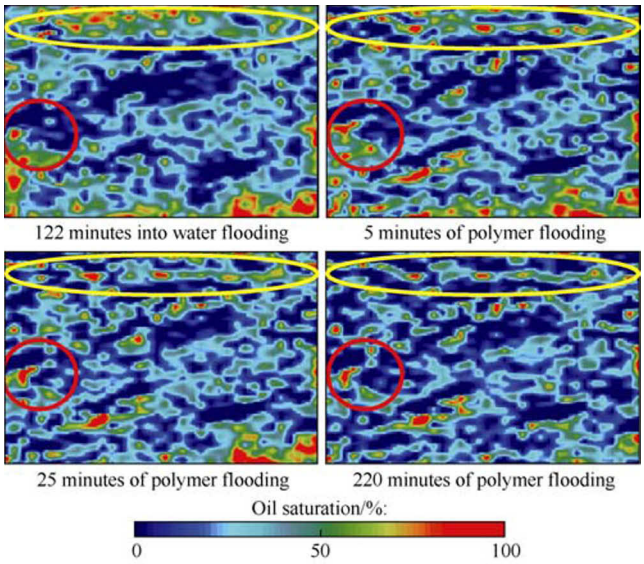

Fig. 10 CT reconstructed images of core LY-1 during polymer flooding

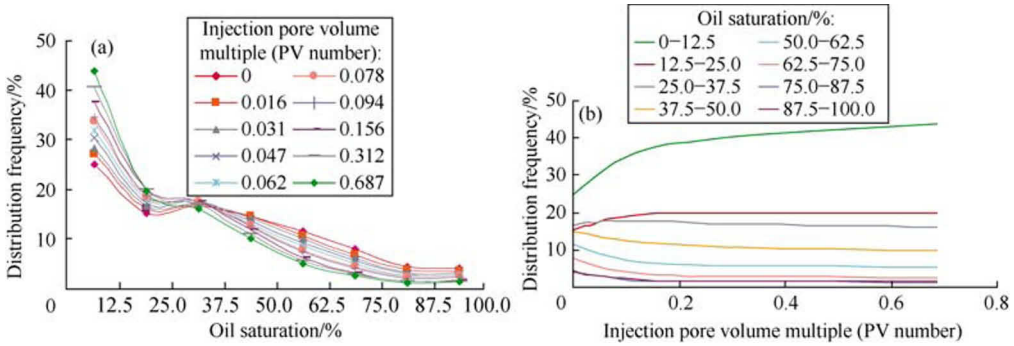

Fig. 11 Oil saturation frequency distribution of LY-1 during polymer flooding

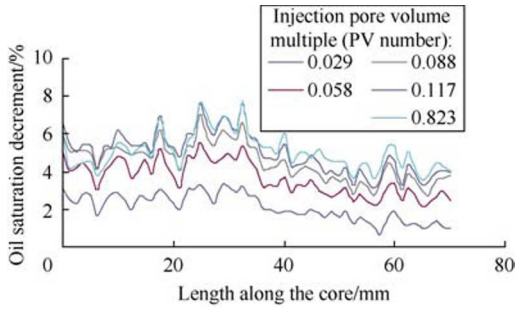

Fig. 12 Oil saturation decrement distribution along the core of LY-2 during 2nd water flooding

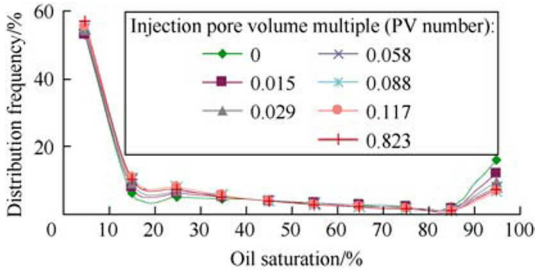

Fig. 13 Oil saturation frequency distribution of LY-2 during 2nd water flooding

Table 2 Recovery percent of LY-1 and LY-2

Sample No	Recovery percent/%			Total recovery percent/%
	1st water flooding	Polymer flooding	2nd water flooding	
LY-1	45.4	19.9	0	66.3
LY-2	35.0	15.6	10.3	60.9

reduced appropriately. Because the polymer in the late stage polymer flooding only pushes the polymer slug formed in the early stage polymer flooding to produce oil, 2nd water flooding can play the role as well and more economically.

The 1st water flooding of LY-2 ended up with a water cut of 90%. The recovery percent of LY-2 after 1st water flooding and polymer flooding was lower than normal. And during the 2nd water flooding there was still quite some oil produced. After a comprehensive analysis of the oil saturation decrement distribution, the CT reconstructed images and the oil saturation frequency distribution, it is inferred that the low water injection degree of 1st water flooding resulted in low recovery percent and massive residual oil in the 'dominant channels' when 1st water flooding ended, which made it difficult to form effective polymer slug, so few new channels were opened during the polymer flooding, and the produced oil in polymer flooding and 2nd water flooding was mainly from the 'dominant channels' and only a small quantity was from new channels formed in the polymer flooding.

In summary, for conglomerate reservoirs with intense heterogeneity, 1st water flooding should reach as high water cut as possible in order to strengthen the plugging effect of polymer. Meanwhile the injection PV number of polymer should be reduced appropriately, since 2nd water flooding can push the slug formed during the polymer flooding to produce oil more efficiently and economically.

5 Conclusions

In the waterflooding of strongly heterogeneous conglomerate, 'dominant channels' were formed in the early stage, and no new channels were opened in the late stage, so the produced oil was all from the 'dominant channels'. There was still much 'isolated' residual oil left unproduced after polymer flooding. During 2nd water flooding, no new channels were opened and only the residual oil in the channels formed before could be produced.

During the 1st water flooding of conglomerate, the oil in the high oil saturation zones was firstly produced, while only a small part of oil in the medium-low oil saturation zone was produced. During polymer flooding, the oil in the high-medium saturation zone could be produced but oil in the low saturation zone was still hard to be produced. During the 2nd water flooding the produced oil was still mainly from the high oil saturation zone.

In view of the situation of conglomerate reservoirs, the 1st water flooding should reach as high water cut as possible, and the polymer injection volume should be reduced appropriately, for the 2nd water flooding can be used to push the polymer slug to produce oil at lower cost.

References

[1] Li Xiongyan, Zhou Jinyu, Li Hongqi, et al. Computational intelligent methods for predicting complex lithologies and multiphase fluids. Petroleum Exploration and Development, 2012, 39(2): 243–248.

[2] Feng Huijie, Nie Xiaobin, Xu Guoyong, et al. Microscopic mechanisms of oil displacement by polymer solution for conglomerate. Oilfield Chemistry, 2007, 24(3): 232–237.

[3] Bai Bin, Zhu Rukai, Wu Songtao, et al. Multi-scale method of Nano(Micro)-CT study on microscopic pore structure of tight sandstone of Yanchang Formation, Ordos Basin. Petroleum Exploration and Development, 2013, 40(3): 329–333.

[4] Lü Weifeng, Leng Zhenpeng, Liu Qingjie, et al. Measurement of oil recovery by GAGD in water-wet and oil-wet conditions. Napa Valley: Society of Core Analysts, 2013.

[5] Leng Zhenpeng, Lü Weifeng, Zhang Zubo, et al. Methods of measuring relative permeability curves with low permeability core based on CT scanning. Special Oil & Gas Reservoirs, 2013, 20(1): 118–121.

[6] Wang S Y, Huang Y B, Pereira V, et al. Application of computed tomography to oil recovery from porous media. Applied Optics, 1985, 24(23): 4021–4027.

[7] Withjack E M, Devier C, Michael G. The role of X-ray computed tomography in core analysis. SPE 83467, 2003.

[8] Christe P, Turberg P, Labiouse P, et al. An X-ray computed tomography-based index to characterize the quality of cata-

clastic carbonate rock samples. Engineering Geology, 2011, 117(3/4): 180–188.

[9] Lü Weifeng, Liu Qingjie, Zhang Zubo, et al. Measurement of three-phase relative permeabilities. Petroleum Exploration and Development, 2012, 39(6): 713–718.

[10] Zhang Zubo, Zhang Guanliang, Lü Weifeng, et al. An experimental study of waterflooding from layered sandstone by CT scanning. Napa Valley: Society of Core Analysts, 2013.

[11] Lü Weifeng, Liu Qingjie, Zhang Zubo, et al. Measurement of three-phase relative permeabilities of various saturating histories and wettability conditions. Aberdeen: Society of Core Analysts, 2012.

[12] Wang Jialu, Gao Jian, Liu Li. Porosity characteristics of sandstone by X-ray CT scanning system. Acta Petrolei Sinica, 2009, 30(6): 887–893, 896.

[13] Lü Weifeng, Leng Zhenpeng, Zhang Zubo, et al. Study on waterflooding mechanism in low-permeability cores using CT scan technology. Petroleum Geology and Recovery Efficiency, 2013, 20(2): 87–90.

[14] Leng Zhenpeng, Lü Weifeng, Ma Desheng, et al. Research of enhancing oil recovery mechanism of GAGD using CT scanning method. Acta Petrolei Sinica, 2013, 34(2): 340–344.